

Supplementary Information for:

Non-stoichiometric Molybdenum Sulfide Clusters and Their Reactions with Hydrogen Molecule

Yan Chen, Jia-Jun Deng*, Wen-Wen Yao, Joseph Israel Gurti, Wei Li, Wen-Jie Wang, Jian-Xi Yao,
and Xun-Lei Ding*

*Authors to whom correspondence should be addressed.

Emails: dingxl@ncepu.edu.cn; djiaj@ncepu.edu.cn

Table of Contents

Table S1. The distance between Mo-Mo atoms in the most stable structure of Mo_xS_y clusters.	(S2)
Table S2. Natural bond orbital analyses for $\text{H}_2 \dots \text{Mo}_x\text{S}_y$ clusters.	(S3)
Figure S1. Calculated low-lying isomers of Mo_2S_y ($y = 2-8$).	(S4)
Figure S2. Calculated low-lying isomers of Mo_3S_y ($y = 3-9$).	(S5)
Figure S3. Calculated low-lying isomers of Mo_4S_y ($y = 4-10$).	(S6)
Figure S4. Relationship between adsorption energy (E_{ad}) and electron transfer (Q) for $\text{H}_2 \dots \text{Mo}_x\text{S}_y$ clusters.	(S7)
Figure S5. Relationship between adsorption energy (E_{ad}) and H-Mo bond length ($d_{\text{H-Mo}}$) for $\text{H}_2 \dots \text{Mo}_x\text{S}_y$ clusters.	(S8)
Figure S6. Relationship between adsorption energy (E_{ad}) and H-H bond length ($d_{\text{H-H}}$) for $\text{H}_2 \dots \text{Mo}_x\text{S}_y$ clusters.	(S9)
Figure S7. Relationship between adsorption energy (E_{ad}) and symmetric H ₂ -Mo vibration ($\nu_{\text{s}}(\text{Mo-H}_2)$) for $\text{H}_2 \dots \text{Mo}_x\text{S}_y$ clusters.	(S10)
Figure S8. Relationship between adsorption energy (E_{ad}) and asymmetric H ₂ -Mo vibration ($\nu_{\text{a}}(\text{Mo-H}_2)$) for $\text{H}_2 \dots \text{Mo}_x\text{S}_y$ clusters.	(S11)
Figure S9. Relationship between adsorption energy (E_{ad}) and H-H vibration ($\nu(\text{H-H})$) for $\text{H}_2 \dots \text{Mo}_x\text{S}_y$ clusters.	(S12)
Calculations on two-dimensional molybdenum sulfide monolayer with grid structure	(S13)

Table S1. Calculated distance between Mo-Mo atoms (d_i) in the most stable structure of Mo_xS_y clusters. \bar{d} is the averaged value of d_i (except $d_i > 380$ pm) for each cluster. All values are in picometer.

Mo_2S_y		Mo_3S_y					\bar{d}
y	d_1	y	d_1	d_2	d_3		
2	210	3	225	225	281	244	
3	204	4	232	232	261	242	
4	265	5	227	269	269	255	
5	279	6	269	269	279	273	
6	299	7	276	294	294	288	
7	319	8	297	297	409	297	
8	276	9	343	343	354	347	
Mo_4S_y							
y	d_1	d_2	d_3	d_4	d_5	d_6	\bar{d}
4	225	249	256	256	256	257	250
5	248	255	255	255	255	259	254
6	257	257	257	257	257	257	257
7	257	257	257	257	257	258	257
8	278	280	280	280	280	487	280
9	274	274	315	315	331	377	315
10	287	287	322	322	325	489	308

Table S2. Natural bond orbital analyses for $H_2 \dots Mo_x S_y$ clusters. δ is the occupancy of NBOs, ΔE^2 (kcal mol⁻¹) is the second-order perturbation energy, BD is the 2-center (c) bond, BD* is the 2c anti-bond, LP is the lone pair 1c valence orbital, LP* is the empty 1c valence orbital, RY is the 1c Rydberg-type orbital, and LV is the energy-sorted lone vacant orbital. For triplet systems, two lines are listed for spin up and down, respectively. All data are calculated with B3LYP-D3/ma-def2-TZVP, except those in the parentheses with def2-TZVP. Results of H₂-23a and H₂-25a indicate that diffuse functions have little effect here.

	H ₂ → Cluster					Cluster → H ₂				
	Donor	δ	Acceptor	δ	ΔE^2	Donor	δ	Acceptor	δ	ΔE^2
H ₂ -22a	BD H-H	0.918	BD* Mo-S	0.117	21.31	LP Mo	0.948	BD* H-H	0.054	7.71
	BD H-H	0.920	BD* Mo-S	0.109	20.87	BD Mo-S	0.867	BD* H-H	0.018	1.47
H ₂ -23a	BD H-H	1.821 (1.821)	BD* Mo-S	0.237 (0.235)	37.19 (37.87)	BD Mo-S	1.911 (1.912)	BD* H-H	0.051 (0.052)	3.60 (3.57)
H ₂ -24a	BD H-H	(0.880)	BD* Mo-S	(0.170)	(19.15)	LP Mo	(0.897)	BD* H-H	(0.046)	(7.48)
	BD H-H	(0.878)	BD* Mo-S	(0.099)	(22.85)	LP Mo	(0.745)	BD* H-H	(0.022)	(8.36)
H ₂ -25a	BD H-H	1.751 (1.752)	BD* Mo-S	0.221 (0.221)	48.34 (48.27)	LP Mo	1.638 (1.638)	BD* H-H	0.064 (0.065)	17.07 (17.30)
H ₂ -33a	BD H-H	0.880	LV Mo	0.218	5.50	LP Mo	0.966	BD* H-H	0.025	3.17
	BD H-H	0.878	LV Mo	0.156	23.13	BD Mo-S	0.911	RY H	0.001	0.86
H ₂ -33b	BD H-H	0.920	BD* Mo-S	0.246	21.67	LP Mo	0.658	BD* H-H	0.084	16.43
	BD H-H	0.918	BD* Mo-S	0.141	20.06	LP Mo	0.559	BD* H-H	0.063	24.27
H ₂ -33b'	BD H-H	0.921	BD* Mo-Mo	0.292	12.24	LP Mo	0.967	BD* H-H	0.036	5.02
	BD H-H	0.922	BD* Mo-Mo	0.285	12.76	BD Mo-Mo	0.841	RY H	0.000	1.11
H ₂ -34a	BD H-H	0.907	RY Mo	0.094	9.67	LP Mo	0.340	RY H	0.004	2.19
	BD H-H	0.902	LV Mo	0.209	17.37	LP Mo	0.277	RY H	0.002	6.15
H ₂ -35a	BD H-H	1.790	BD* Mo-S	0.316	35.59	LP Mo	1.023	RY H	0.003	16.59
H ₂ -36a	BD H-H	1.759	BD* Mo-S	0.257	50.75	LP Mo	1.616	BD* H-H	0.061	19.67
H ₂ -44a	BD H-H	0.922	BD* Mo-Mo	0.281	6.27	BD Mo-Mo	0.759	RY H	0.002	17.34
	BD H-H	0.921	BD* Mo-Mo	0.163	8.26	BD Mo-Mo	0.747	RY H	0.002	7.77
H ₂ -45a	BD H-H	1.845	BD* Mo-Mo	0.360	19.24	BD Mo-Mo	1.739	BD* H-H	0.009	2.87
H ₂ -45a'	BD H-H	1.845	LV Mo	0.874	28.84	LP Mo	1.448	BD* H-H	0.009	4.36
H ₂ -46a	BD H-H	1.846	BD* Mo-Mo	0.352	13.51	BD Mo-Mo	1.502	RY H	0.003	5.69
H ₂ -47a	BD H-H	1.849	BD* Mo-Mo	0.377	31.47	RY S	0.882	RY H	0.005	13.98
H ₂ -47a'	BD H-H	1.775	BD* Mo-Mo	0.452	12.84	RY S	0.975	RY H	0.003	13.97
H ₂ -48a	BD H-H	1.764	BD* Mo-S	0.301	53.23	RY Mo	0.890	RY H	0.004	21.21

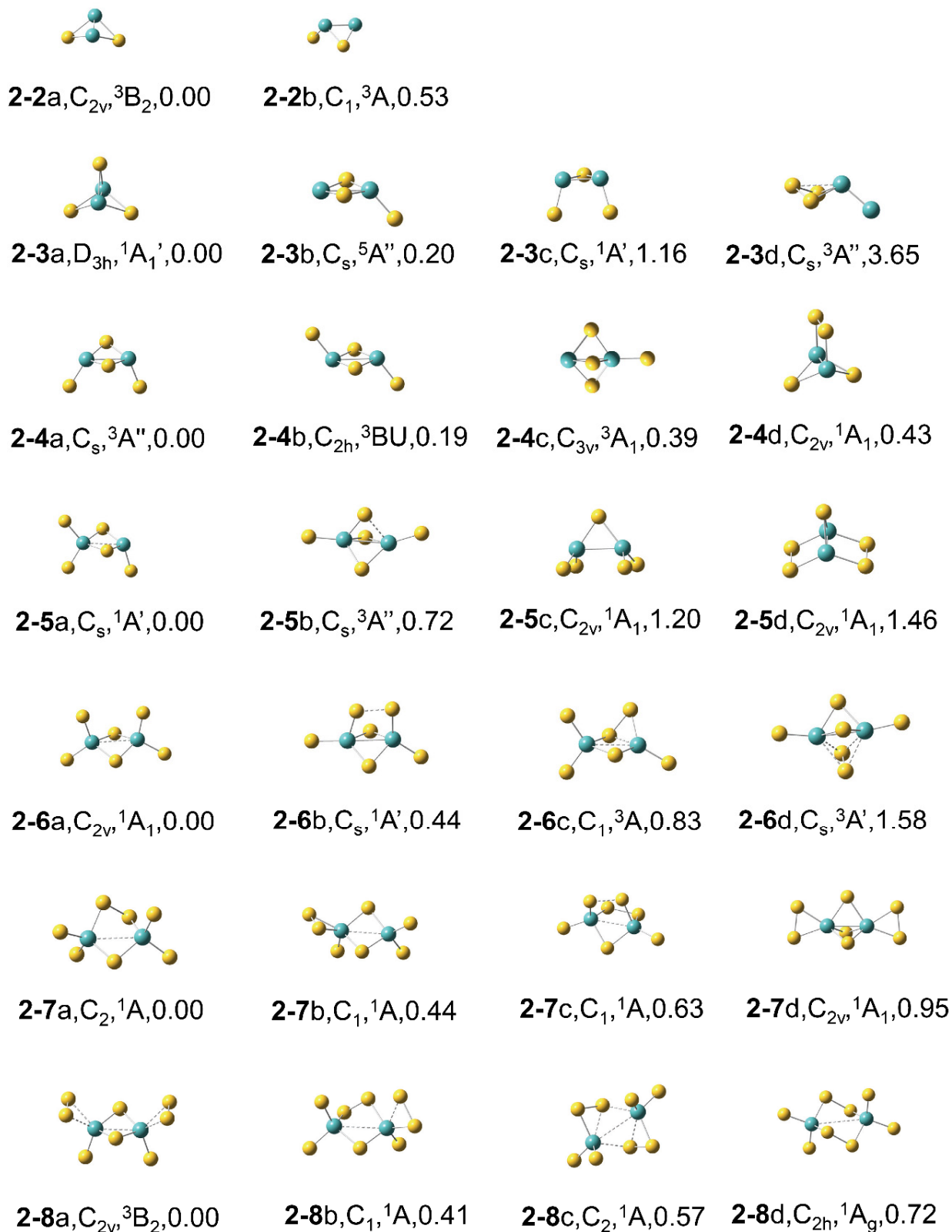


Figure S1. Calculated low-lying isomers of Mo_2S_y ($y = 2-8$). Dashed lines denote Mo-Mo bonds of 275-380 pm, Mo-S bonds of 244-275 pm, or S-S bonds of 214-237 pm. The symmetry, electronic state, and relative energy (in eV) with respect to the ground state are listed below each structure.

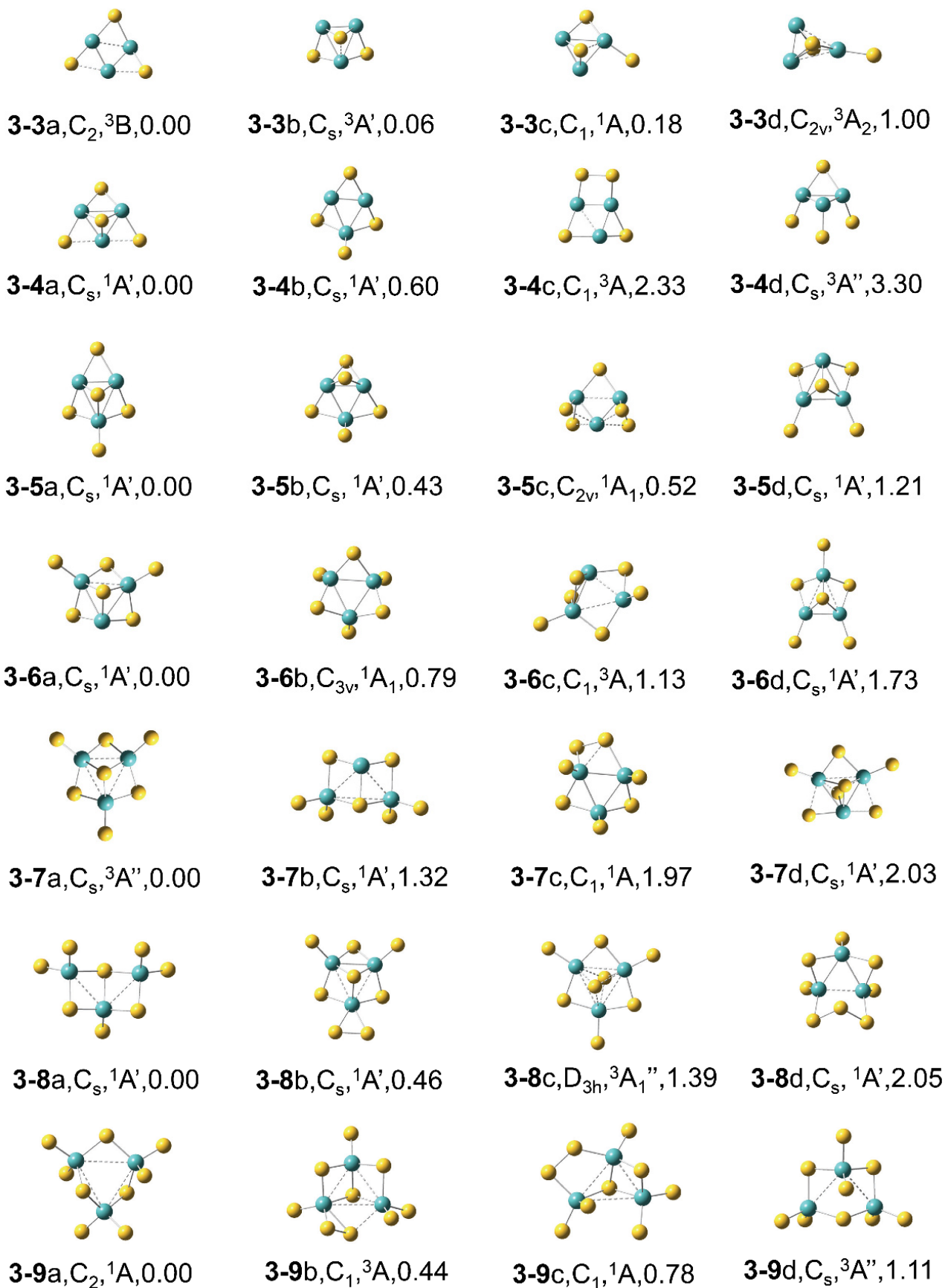


Figure S2. Calculated low-lying isomers of Mo_3S_y ($y = 3-9$). See the caption of Figure S1 for more details.

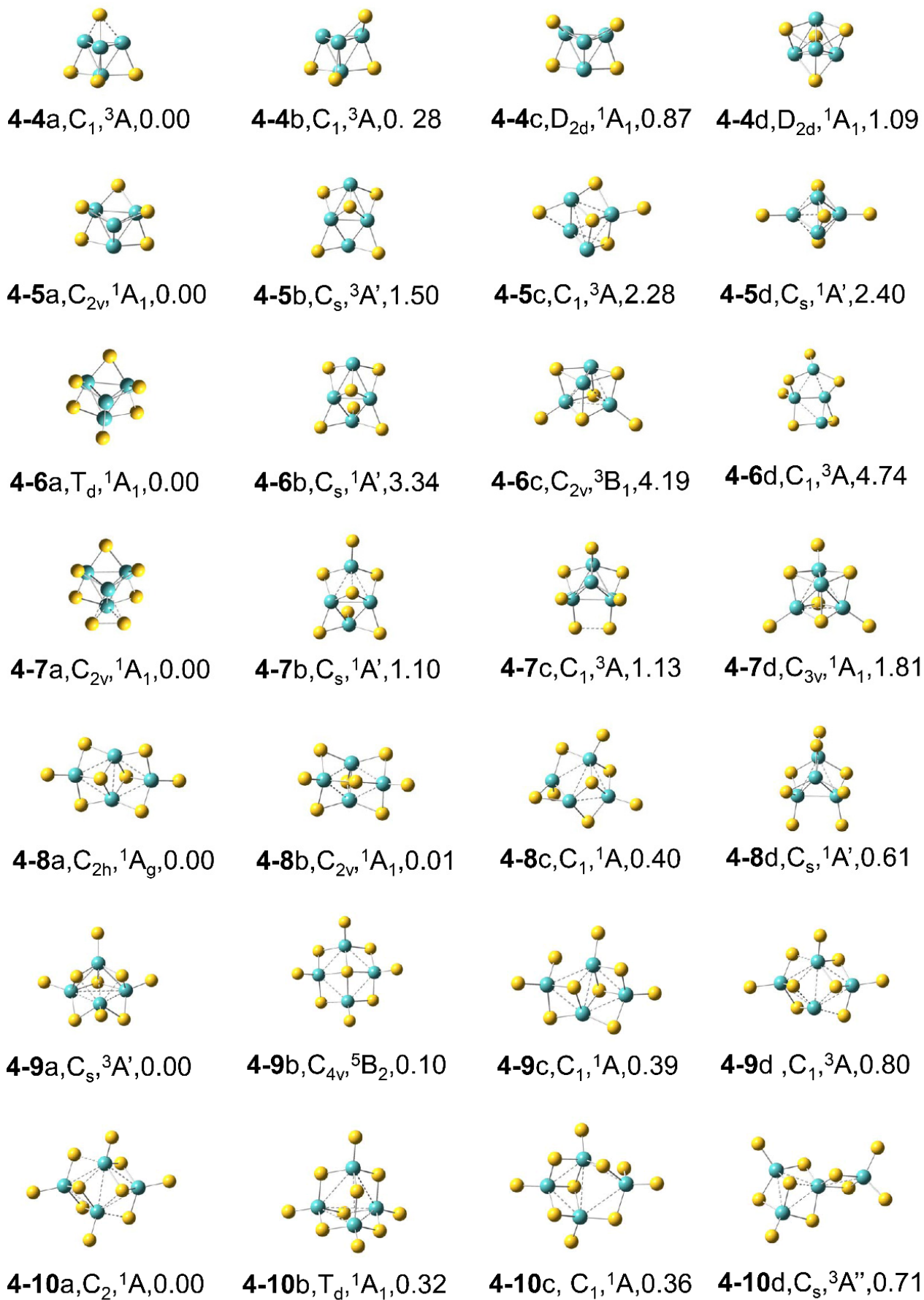


Figure S3. Calculated low-lying isomers of Mo_4S_y ($y = 4-10$). See the caption of Figure S1 for more details.

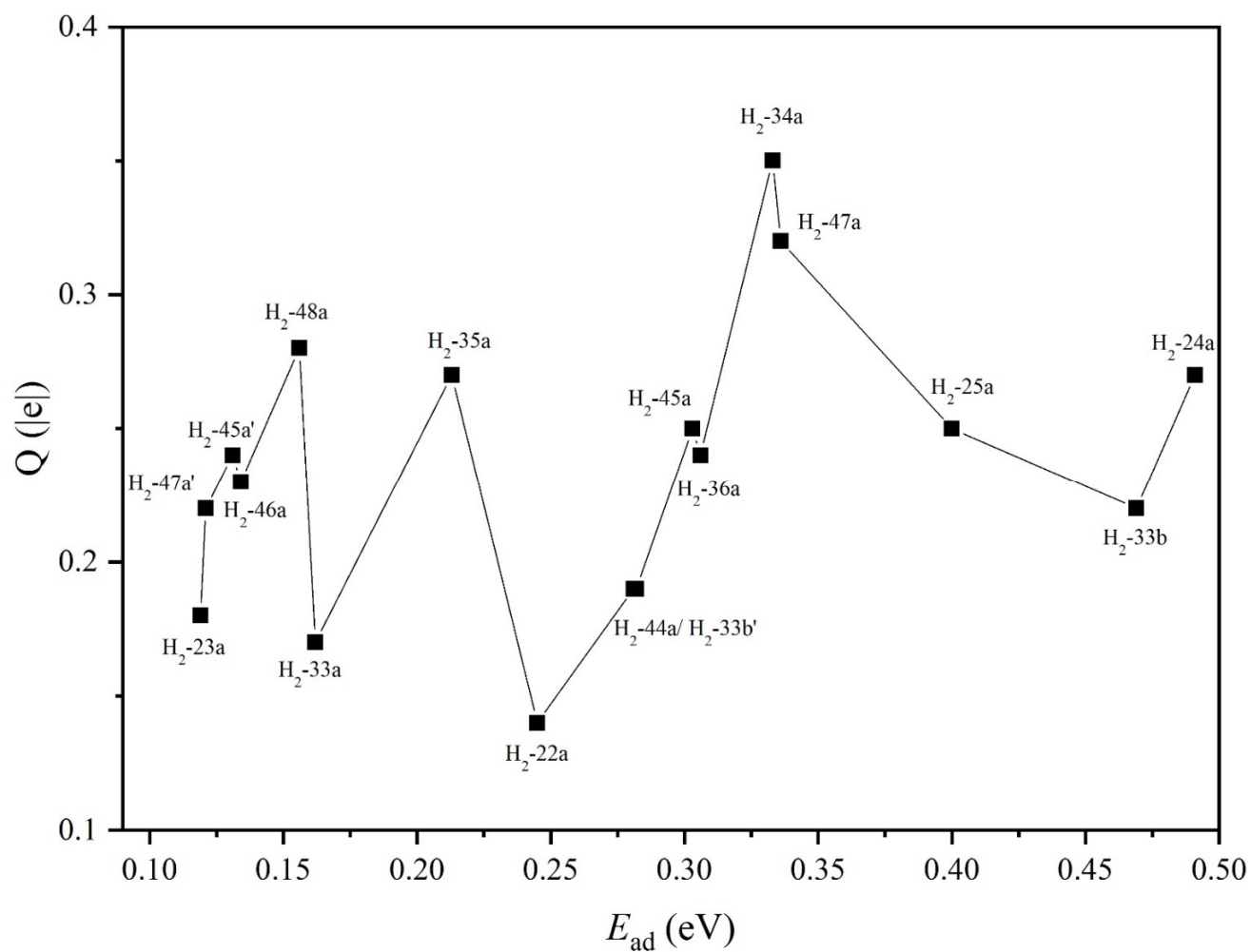


Figure S4. Relationship between adsorption energy (E_{ad}) and electron transfer (Q) for $H_2 \dots Mo_x S_y$ clusters.

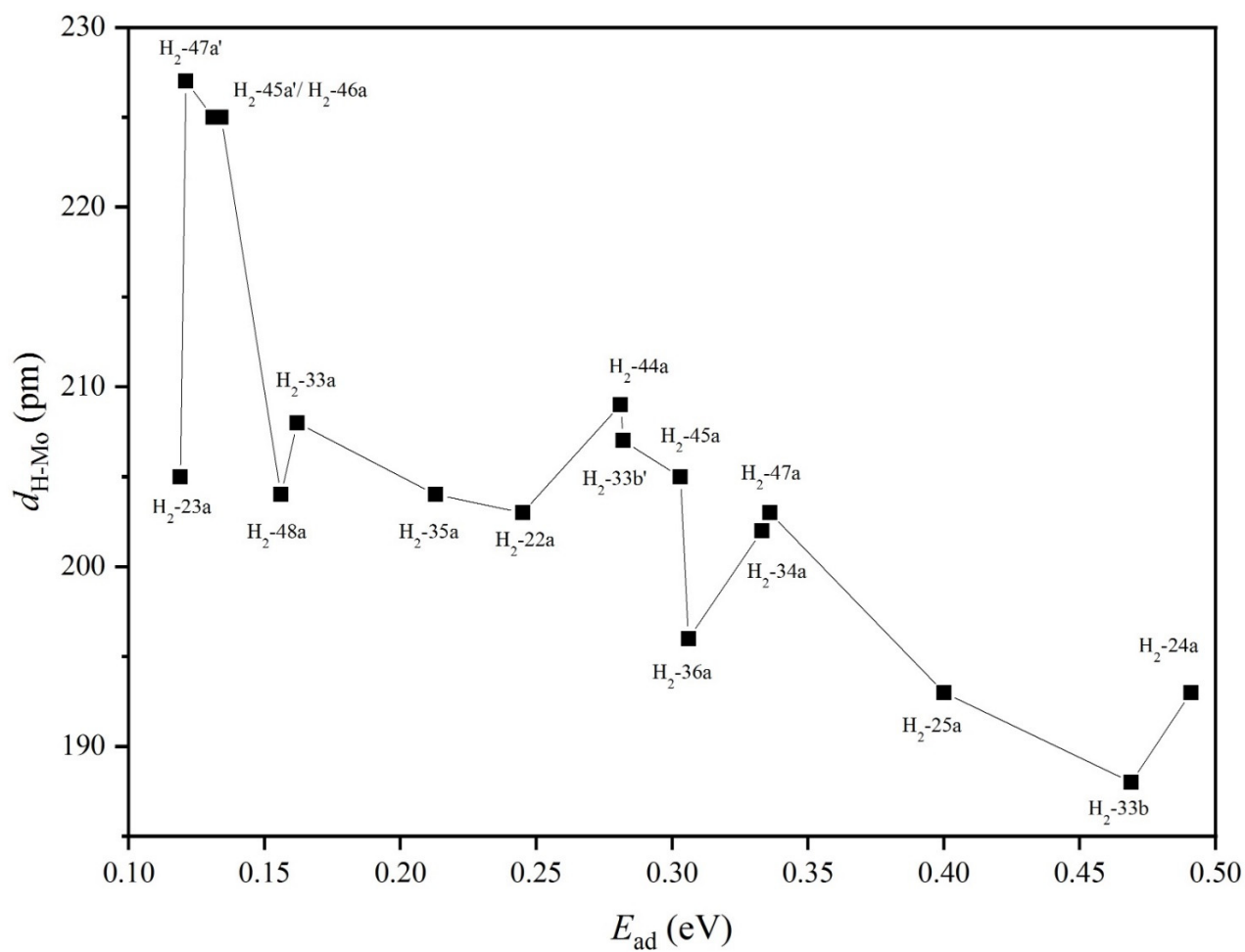


Figure S5. Relationship between adsorption energy (E_{ad}) and H-Mo bond length (d_{H-Mo}) for H₂...Mo_xS_y clusters.

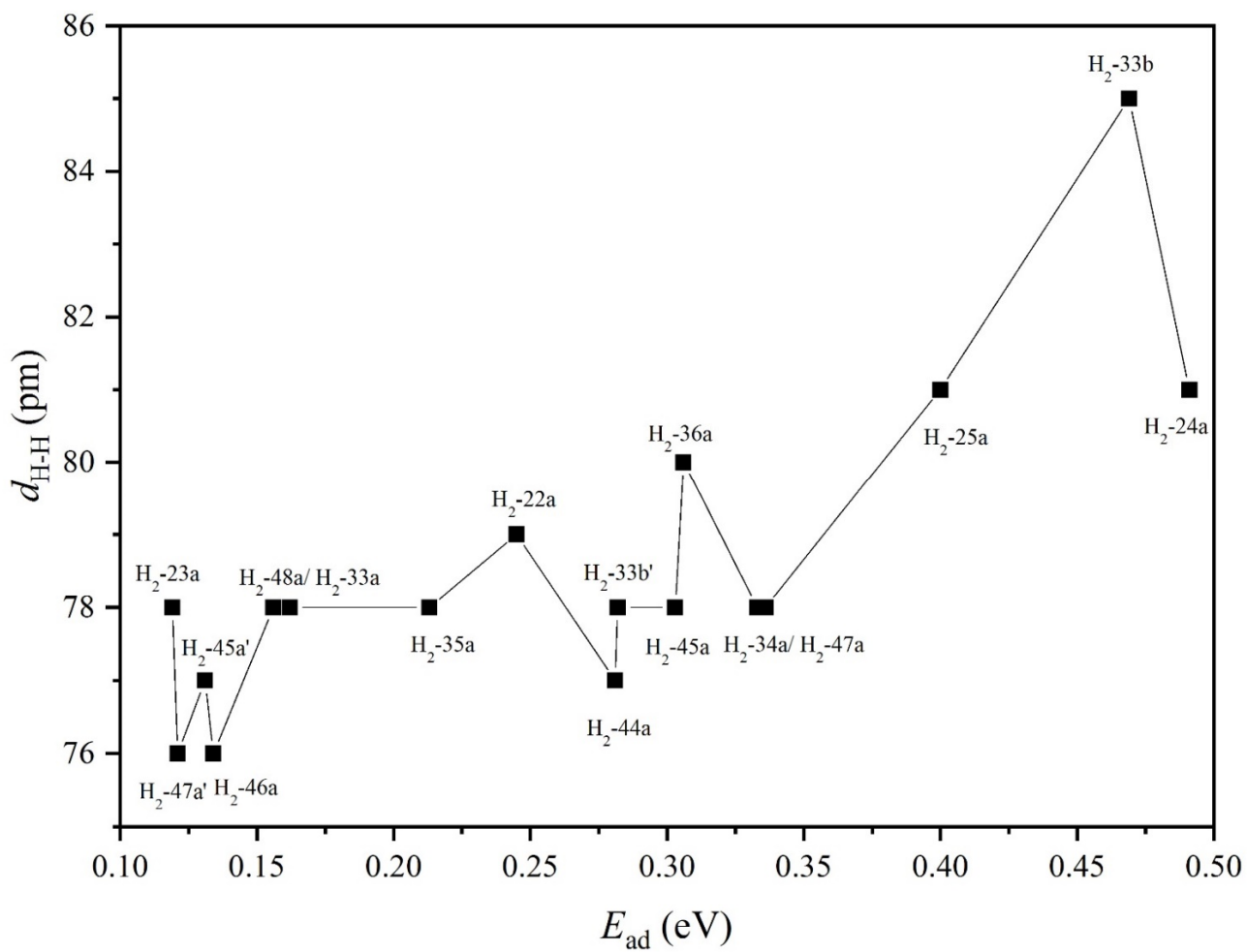


Figure S6. Relationship between adsorption energy (E_{ad}) and H-H bond length (d_{H-H}) for H₂...Mo_xS_y clusters.

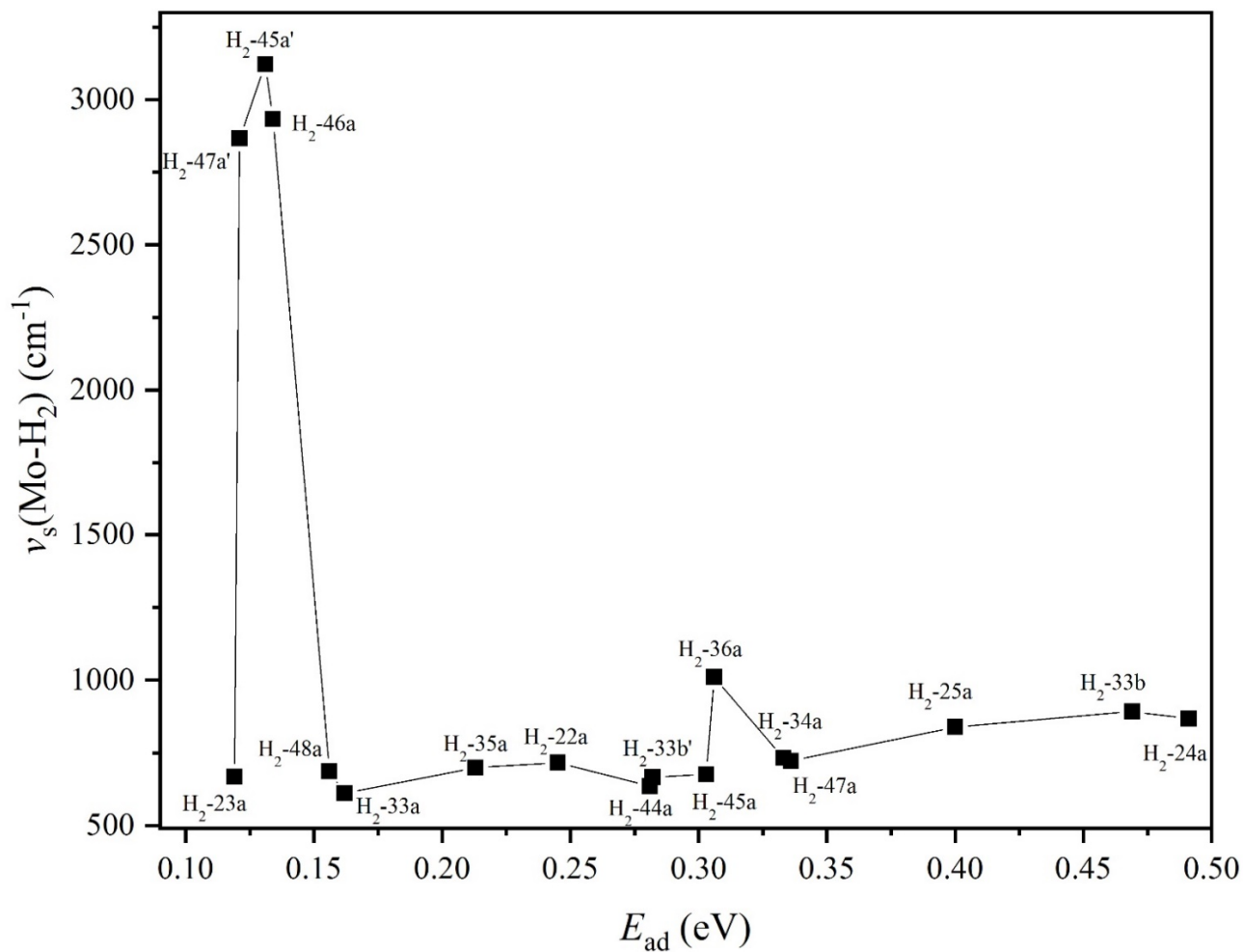


Figure S7. Relationship between adsorption energy (E_{ad}) and symmetric H₂-Mo vibration ($\nu_s(\text{Mo-H}_2)$) for H₂...Mo_xS_y clusters.

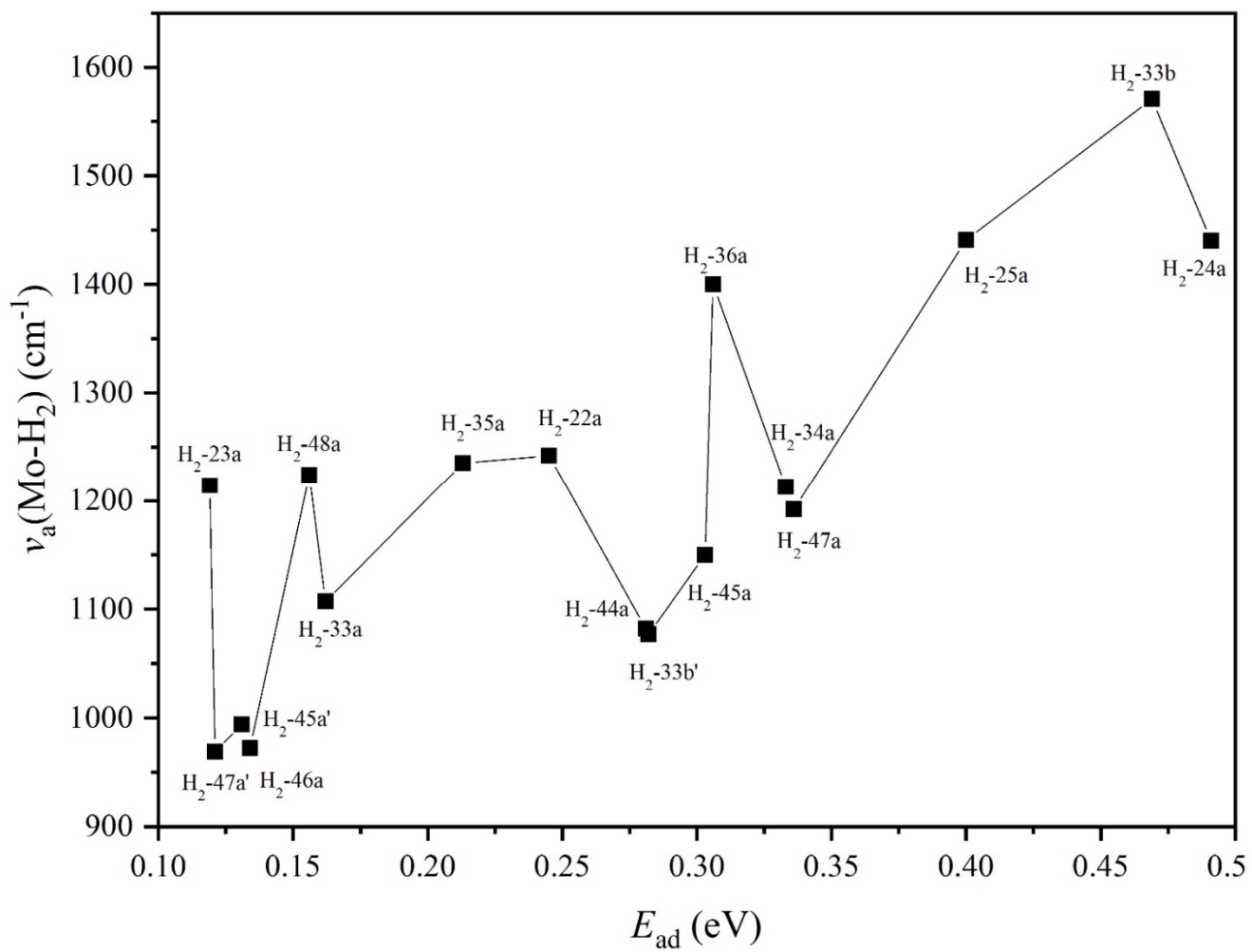


Figure S8. Relationship between adsorption energy (E_{ad}) and asymmetric H₂-Mo vibration ($\nu_a(\text{Mo-H}_2)$) for H₂...Mo_xS_y clusters.

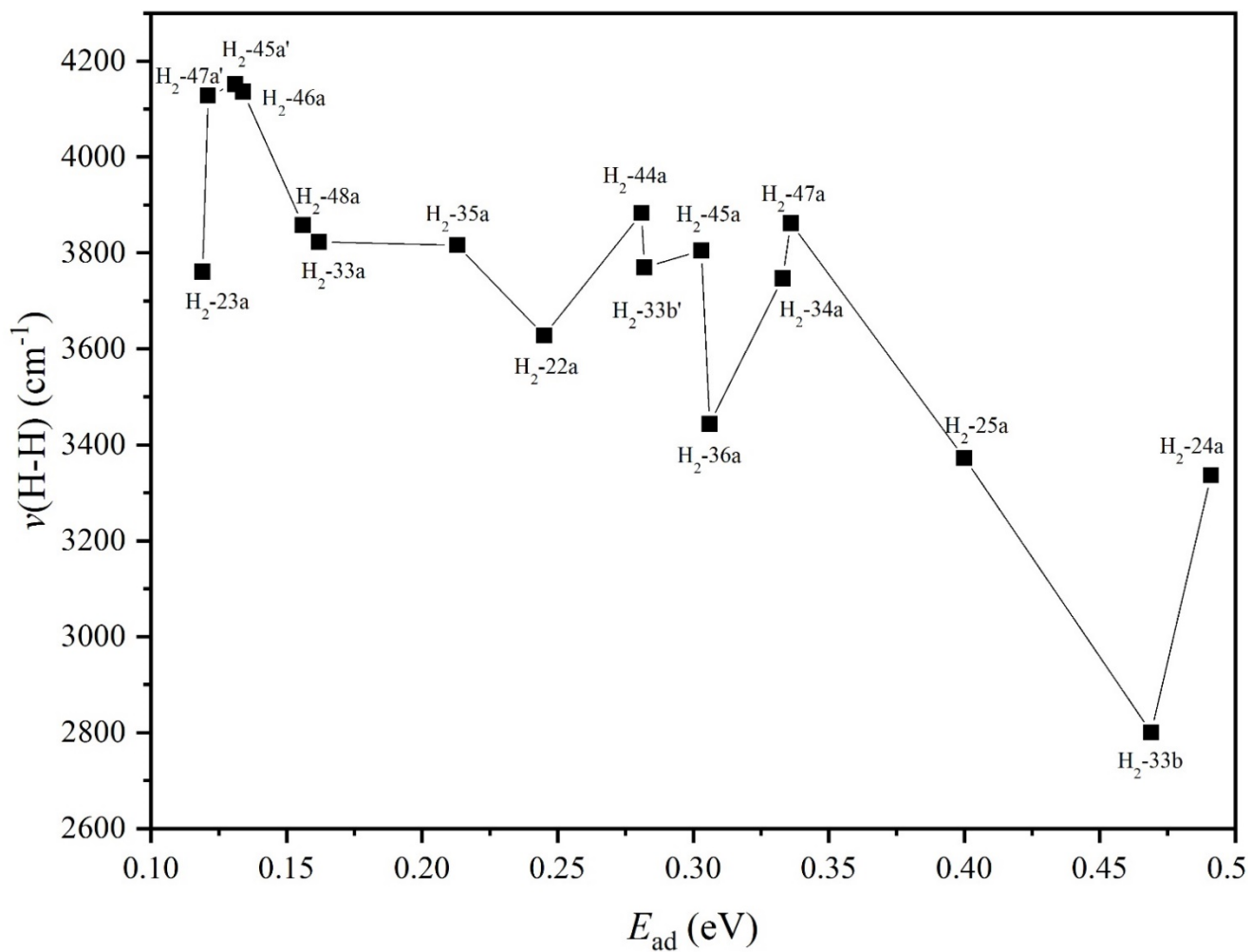


Figure S9. Relationship between adsorption energy (E_{ad}) and H-H vibration ($\nu(\text{H-H})$) for H₂...Mo_xS_y clusters.

Calculations on two-dimensional molybdenum sulfide monolayer with grid structure

We performed DFT calculations on the two-dimensional grid structure using Vienna Ab initio Simulation Package (VASP).^{1,2} The Perdew-Burke-Ernzerhof (PBE) generalized gradient approximation (GGA) functional with the projector augmented-wave method³⁻⁵ was used and all calculations were performed in a spin unrestricted manner. The square grid with two Mo and two S atoms is chosen as the unit cell to build the periodic two-dimensional slab along a and b directions (Figure S7), and a vacuum of about 15 Å is added between two slabs to eliminate the interactions between repeated slabs. The energy cutoff for the plane-wave basis expansion was chosen to be 500 eV. We sampled $6 \times 6 \times 1$ k-point grid for the integration of the Brillouin zone for the optimization and frequency calculations.

The optimized lattice constant is 374 pm, corresponding to the Mo-Mo distances as 265 pm, which is close to that in our calculations for clusters (280 pm). Zone centered (Γ -point) vibrational frequencies are calculated for the optimized structures. Nine positive frequencies ranging from 142 to 417 cm^{-1} have been obtained, with three negligible virtual frequencies whose absolute values are less than 1 cm^{-1} , which indicates that this type of grid structure has structural stability.

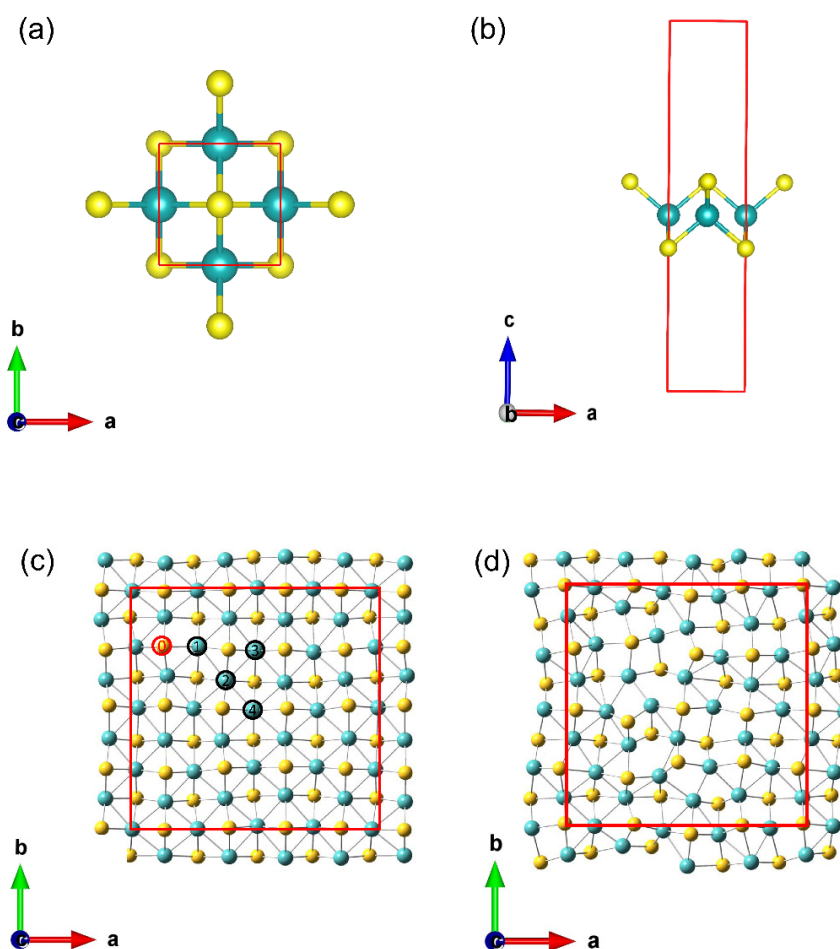


Figure S10. Structures of molybdenum-sulfur single layer slab. Top view (a) and side view (b) after optimization. The last frame of the molecular dynamics simulation under 300 K (c) and 1200 K (d).

Ab initio molecular dynamics (AIMD) simulations are conducted with the unit cell $4 \times 4 \times 1$ times of the unit cell in the optimization calculations. To make AIMD calculations computationally efficient, we used a low cutoff of 250 eV, and the k-point sampling was restricted to the Γ point only. Normal precision in VASP was used with a tolerance of 1×10^{-5} eV for energy convergence in the SCF cycle. The time step is set to 1.0 fs and total time is 10 ps. MD simulations are carried out at 300, 500, 800, 1000, and 1200 K with the NVT ensemble. The structure remains unchanged at low temperature (300 K, Figure S7 c), while at high temperature, it is distorted (1200 K, Figure S7 d), indicating that the structure will be unstable at high temperature. The energy variation is quite small at low temperatures while it becomes large at high temperatures (Figure S8). We examined the radial distribution function of Mo-S distances at different temperatures (Figure S9). At 300 K, it clear that there are four peaks, corresponding to the distances for (S, Mo) pair (0, 1), (0, 2), (0, 3), and (0, 4) (labelled in Figure S7 c), respectively. As temperature increases, these peaks height decreases and their width increases, indicating that the regular structure is gradually broken. The root mean square deviation (RMSD) with respect to the optimized structure was also analysed. RMSD is defined as $RMSD(N; x, y) = \sqrt{(\sum_{i=1}^N \|x_i - y_i\|^2)/N}$, in which N is the atom number in the unit cell; x_i and y_i are the Cartesian coordinates of the i^{th} atom of frame x and the optimized structure y , respectively. The values of RMSD (Figure S10) are quite small (~ 0.2 Å) and steady at 300 K, while they could be large (~ 0.5 Å) and oscillate obviously at 1200 K. This further confirms that the two-dimensional grid structure is stable under room temperature.

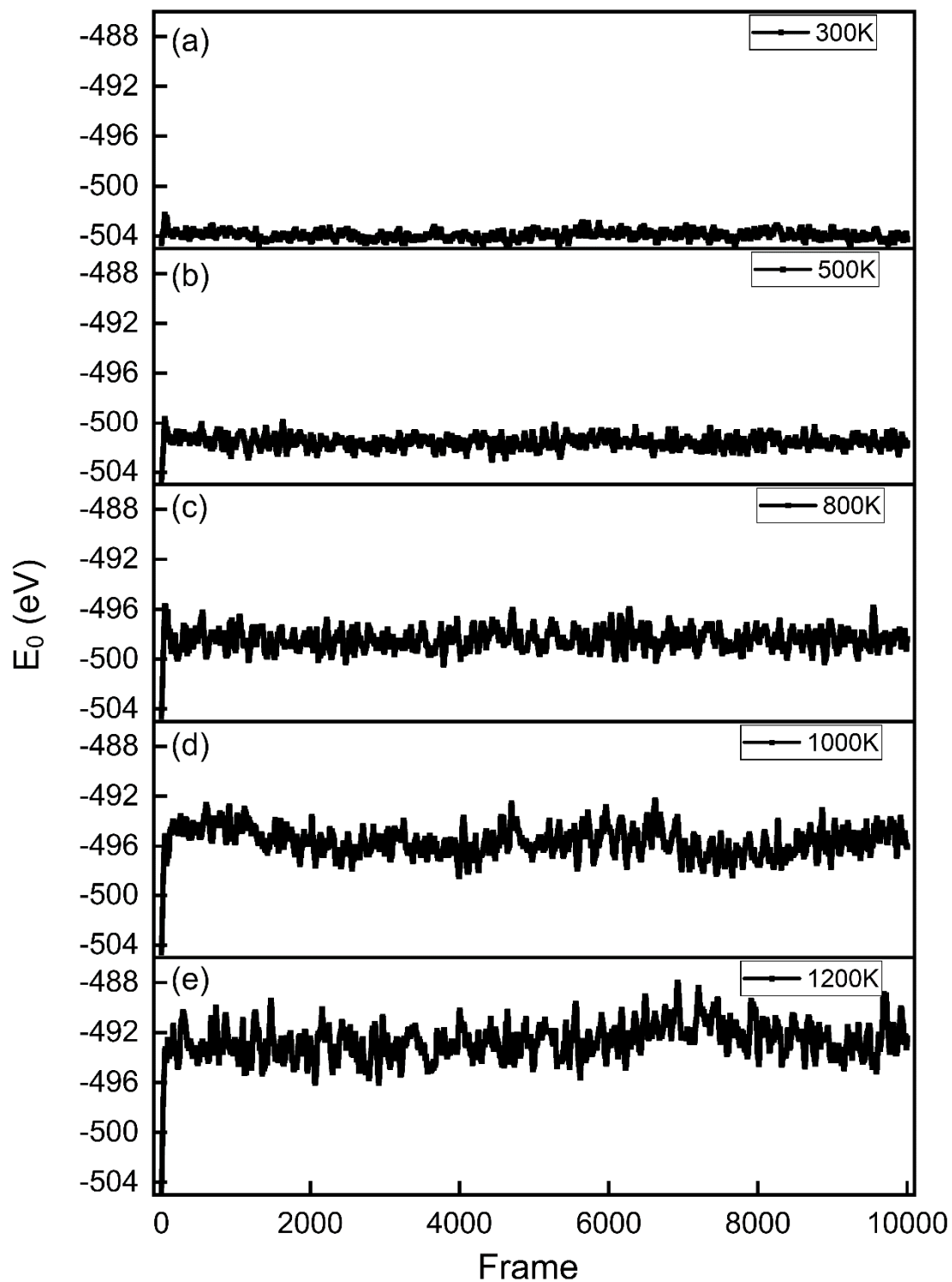


Figure S11. The energy variation of the 10000 frames under (a) 300, (b) 500, (c) 800, (d) 1000, and (e) 1200 K, respectively.

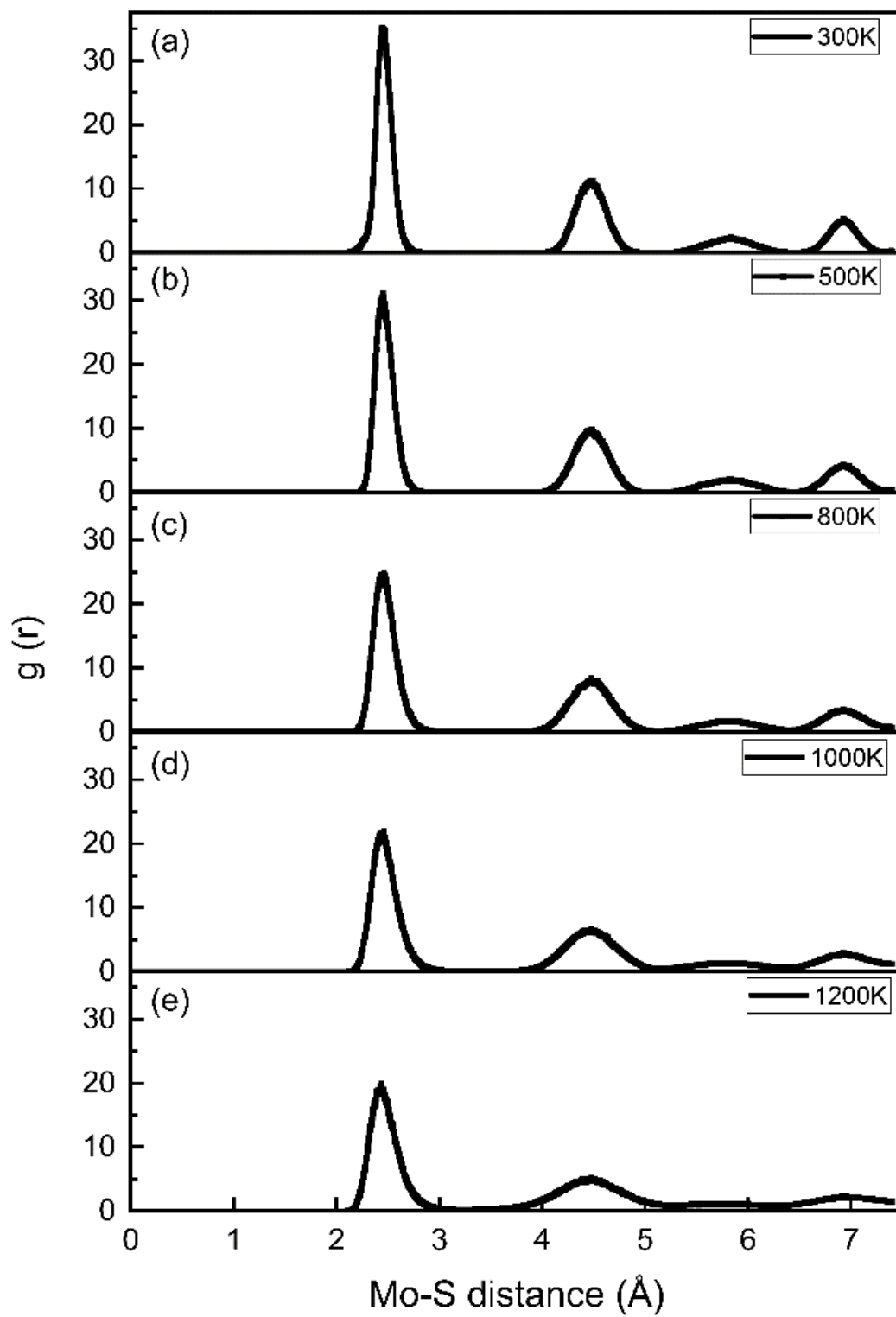


Figure S12. The radial distribution function $g(r)$ of the 10000 frames under (a) 300, (b) 500, (c) 800, (d) 1000, and (e) 1200 K, respectively.

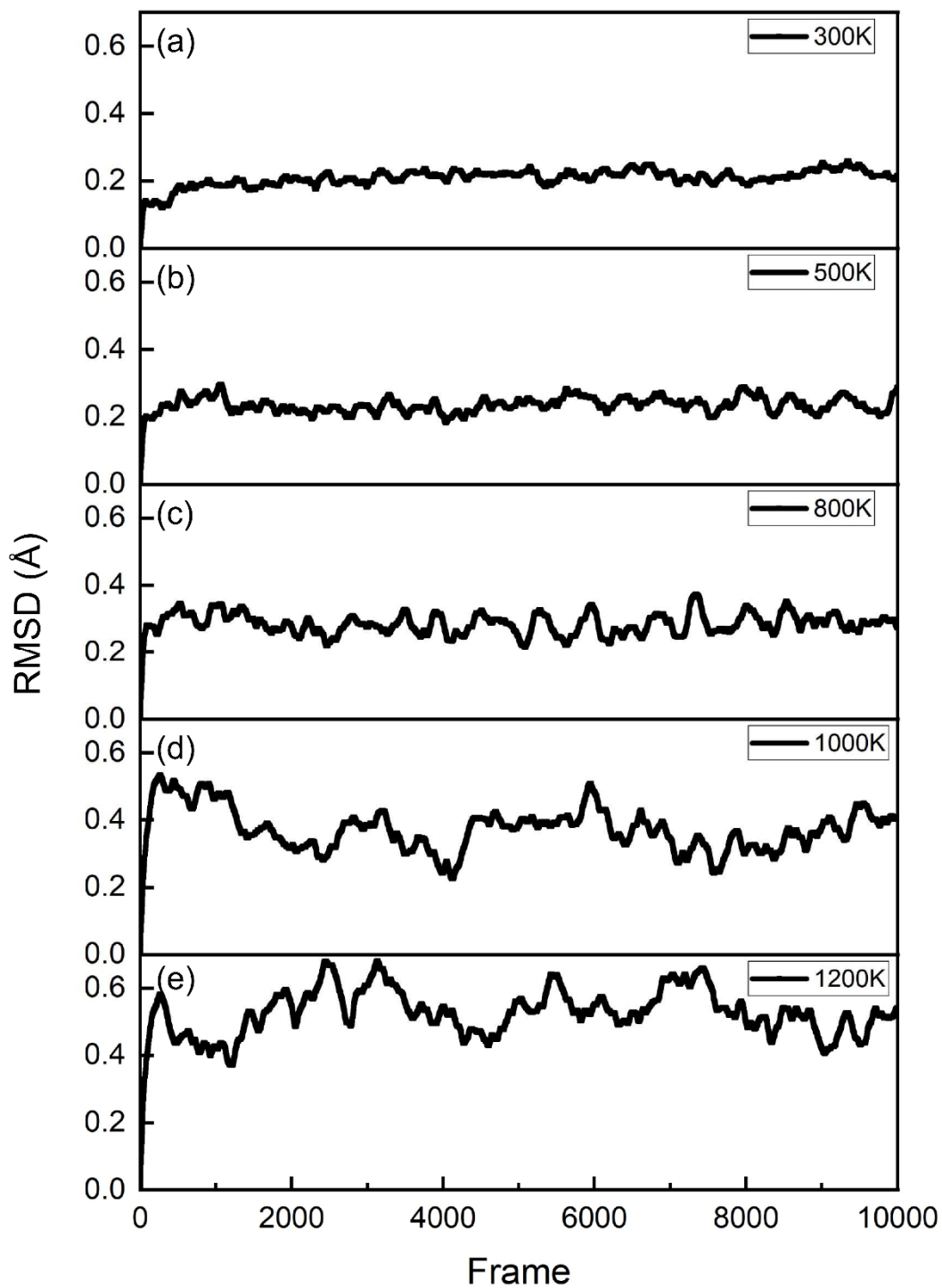


Figure S13. The root mean square deviation of the 10000 frames under (a) 300, (b) 500, (c) 800, (d) 1000, and (e) 1200 K, respectively.

References

- 1 G. Kresse and J. Furthmüller, *Comp. Mater. Sci.*, 1996, **6**, 15.
- 2 G. Kresse and J. Furthmüller, *Phys. Rev. B*, 1996, **54**, 11169.
- 3 G. Kresse and D. Joubert, *Phys. Rev. B*, 1999, **59**, 1758.
- 4 J. P. Perdew, K. Burke and M. Ernzerhof, *Phys. Rev. Lett.*, 1996, **77**, 3865.
- 5 P. E. Blöchl, *Phys. Rev. B*, 1994, **50**, 17953.